Tetrahedron 65 (2009) 9428–9435

Contents lists available at ScienceDirect

Tetrahedron

journal homepage: www.elsevier.com/locate/tet

The effect of spiroadamantane substitution on the conformational preferences of *N*-Me pyrrolidine and *N*-Me piperidine: a description based on dynamic NMR spectroscopy and ab initio correlated calculations

Antonios Kolocouris *

Faculty of Pharmacy, Department of Pharmaceutical Chemistry, University of Athens, Panepistimioupolis-Zografou, 15771 Athens, Greece

ARTICLE INFO

Article history:
Received 28 May 2009
Received in revised form 10 August 2009
Accepted 28 August 2009
Available online 1 September 2009

Keywords:
NMR
^{13}C
^{1}H
Dynamic NMR spectroscopy
Enantiomerization
Spiroadamantane *N*-methylpyrrolidine
Spiroadamantane *N*-methylpiperidine
Ab initio calculations
Nitrogen inversion
Ring inversion

ABSTRACT

Dynamic NMR spectroscopy and ab initio correlated calculations revealed that the attachment of a spiroadamantane entity at the C-2 position of *N*-methylpyrrolidine or *N*-methylpiperidine induces a severe steric crowding around nitrogen, which changes the conformational space of the heterocycle resulting in: (a) the complete destabilization of the *N*-Me(eq) conformer in spiranic structures; in contrast the *N*-Me(eq) conformer corresponds to the global minimum in *N*-methylpyrrolidine or *N*-methylpiperidine. The spiroadamantane structure raises the energy of the equatorial conformer because of the severe van der Waals repulsion between the *N*-Me(eq) group and adamantane C–H bonds. (b) The interconversion between the only populated enantiomeric *N*-Me(ax) conformers ax→[eq]→ax′; the interconversion eq→ax between *N*-Me(eq) and *N*-Me(ax) conformers, which are both populated, is observed in *N*-methylpyrrolidine or *N*-methylpiperidine. (c) The raising of ring and nitrogen inversion barriers ax→ts by ~4–6 kcal mol^{-1}. The dynamic NMR study provides evidence that the most important process required for the enantiomerization between the axial *N*-Me conformers in spiropiperidine **4** and spiropyrrolidine **5** are different, i.e., a nitrogen inversion in **5** (9.10 kcal mol^{-1}) and a ring inversion in **4** (15.2 kcal mol^{-1}). While an enantiomerization interconverts *N*-Me axial conformers in spiropiperidine **5** and spiropyrrolidine **4**, substitution of the pyrrolidine ring of **5** with a *C*-Me group effects a diastereomerization between two *N*-Me axial conformers and reduces effectively the nitrogen inversion barrier according to the protonation experiments and the calculations. In general, all the calculations levels used, i.e., the MM3, B3LYP/6-31+G** and MP2/6-311++G**//B3LYP/6-31+G**, predict correctly the different stability of the local minima; however only MP2/6-311++G**//B3LYP/6-31+G** was found to be reliable for the calculation of the nitrogen inversion barriers.

1. Introduction

Aminoadamantane derivatives represent a class of compounds with interesting biological properties; amantadine **1** and rimantadine **2** are anti-influenza virus A drugs that block the M2 protein ion channel[1] and memantine **3** is an important NMDA receptor antagonist[2] (Scheme 1). In addition to the synthesis of many potent aminoadamantane derivatives,[3] we recently undertook studies on how these molecules interact with the M2TM protein receptor.[4] Some derivatives have restricted internal motions, so the information obtained from structure calculations and dynamic NMR spectroscopy is needed in order to comprehend the conformational profile of these molecules;[5,6] the conformational preferences of the ligands are important for our on going ligand–receptor docking calculations.[7]

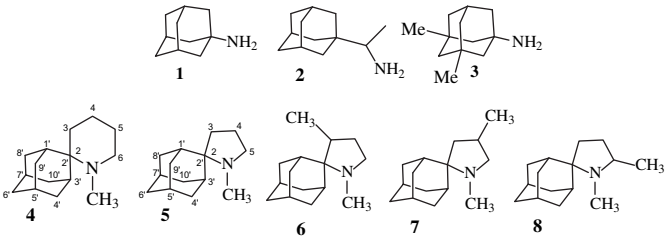

Scheme 1. Prototype aminoadamantane drugs **1–3** and *N*-Me pyrrolidine and *N*-Me piperidine spiroadamantane heterocycles **4–8**.

Compounds **4**,**5** shown in Scheme 1, and their N–H parent molecules, are potent anti-influenza virus A compounds and exhibited NMDA receptor antagonist activity;[3a–d] for example, compound **5** proved to be 350-fold more potent than amantadine **1** against a specific influenza virus A strain.[3a]

In a previous publication the dynamic NMR behaviour of the *N*-methylspiro[piperidine-2,2′-adamantane] **4** was studied;[5] ring

* Tel.: +301 210 7274834; fax: +301 210 7274747.
E-mail address: ankol@pharm.uoa.gr.

0040-4020/$ – see front matter © 2009 Elsevier Ltd. All rights reserved.
doi:10.1016/j.tet.2009.08.071

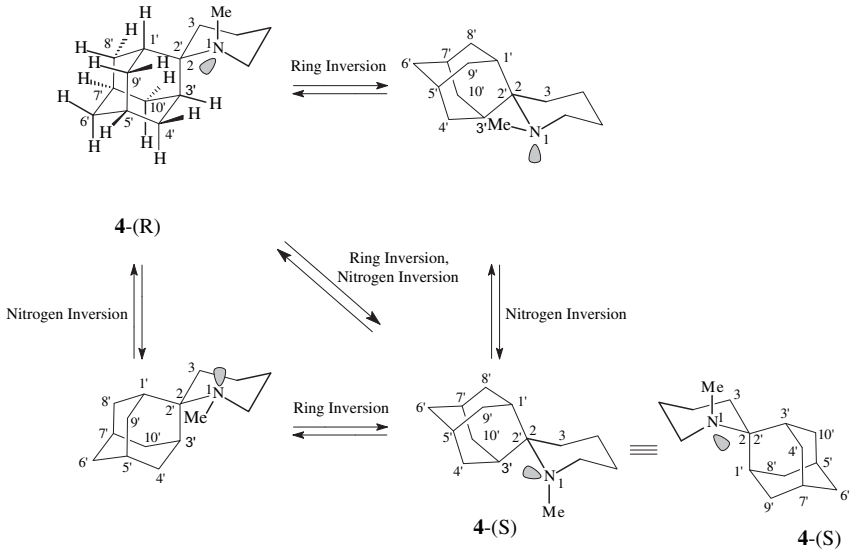

Scheme 2. Interconversion of conformational enantiomers for *N*-methylspiropiperidine **4**.

inversion (RI) and nitrogen inversion (NI) interconvert two conformational enantiomers with an axial *N*-methyl group orientation (Scheme 2). The molecular mechanics MM^{+} calculations[5] located only one populated conformation for compound **4** having a chair piperidine ring conformer and an axial *N*-methyl group (Scheme 2); the calculations predicted that all the other conformers, which include the chair piperidine, *N*-Me(eq) conformer and the twist-boat structures, have more than 4 kcal mol^{-1} higher energy and they are unpopulated.[5] Thus, the typical conformational square in Scheme 2 is contracted to include only the enantiomers **4**-(*R*) and **4**-(*S*).

The enantiomerization process ax→[eq]→ax′ for **4** becomes slow at 273 K (300 MHz) and clear NMR signals of the different pairs of permuted protons 1′,3′-H and $4'_{ax}$,$9'_{ax}$-H and $8'_{ax}$,$10'_{ax}$-H,[8] etc. (see Scheme 2) were observed at that temperature.[5] It can be assumed that the process proceeds through a ring inversion of the *N*-Me(ax) conformer **4**-(*R*) to the unstable *N*-Me(eq) conformer, followed by an N-inversion to the conformational enantiomer **4**-(*S*) (Scheme 2). The experimental free energy of activation for this enantiomerization was found to be $\Delta G^{\#}_{311\ K}$=15.2 kcal mol^{-1}. By intuition it was expected an energy demanded nitrogen inversion barrier for the interconversion *N*-Me(ax)→*N*-Me(eq) in **4**, caused by the *N*-methyl group passing over C1′–C2′ bond of the spiroadamantane entity; several studies have been focused on high energy N-inversion barriers, as it is the 15 kcal mol^{-1} barrier in the 7-methyl-7-azabicyclo[2.2.1]heptane.[9] However, the molecular mechanics calculations placed the NI transition state ~10 kcal mol^{-1} above the ground state chair piperidine ring, *N*-Me(ax) conformer, suggesting that NI is not the slow step and RI was proposed to be the rate determining step for the enantiomerization process.[10] Nevertheless, this value is questioned due to the shortcomings of force field calculations in predicting such conformational barriers.

In the present work, there will be further analysis on how the attachment of a spiroadamantane entity at the C-2 position affects the conformational features of *N*-methylpyrrolidine and *N*-methylpiperidine heterocycles; in a previous work the effect of a 1- or 2-adamantyl substitution was studied.[6] The conformational profile of the spiropyrrolidine **5** will be investigated and will be compared with that of the spiropiperidine **4**. For the *N*-methylspiro[pyrrolidine-2,2′-adamantane] **5** two conformational enantiomers with the *N*-Me group in an axial position can be interconverted through RI (pseudorotation) and NI (Scheme 3), the last being the rate determining process including a transition state (ts) with a planar nitrogen geometry; the preliminary molecular mechanics MM^{+} or MM3 calculations predicted that the *N*-Me(ax) conformation is 6.56 or 5.25 kcal mol^{-1} above the *N*-Me(eq) conformer (which is destabilized due to the repulsive van der Waals forces[11] between the *N*-Me group and adamantane ring), and thus, the only populated. The dynamic NMR results for the *N*-methylspiropyrrolidine **5** are reported here aiming at measuring the NI barrier for the process *N*-Me(ax)→*N*-Me(eq), which approximates to the relevant NI barrier height for the *N*-methylspiropiperidine **4**; the two compounds maintain similar geometrical characteristics around nitrogen for ground state and NI transition state. We recall that according to dynamic NMR spectroscopy the experimental N-inversion barrier eq→ts for *N*-methylpiperidine and *N*-methylpyrrolidine is 8.7 and 7.2 kcal mol^{-1}, respectively.[12,13] It will be presented that the calculations of the NI barriers at the appropriate level of theory can approximate well the experimental values, allowing us to study further how the *C*-methyl substitution in compounds **6**–**8** influences the nitrogen inversion barrier of the spiranic *N*-methylpyrrolidine ring; *C*-methyl substitution of *N*-methylspiropiperidine **4** allows an equilibrium between conformational diastereomers (Scheme 4, Scheme S1 in Supplementary data).

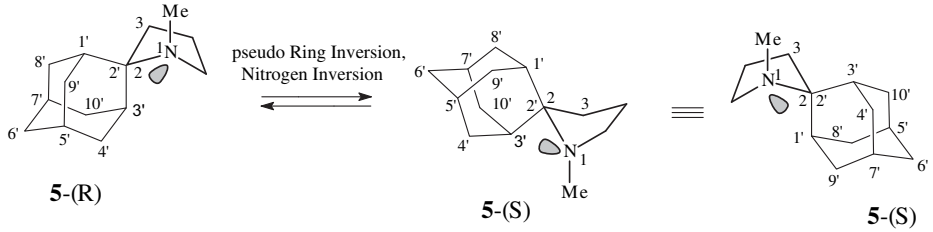

Scheme 3. Interconversion of conformational enantiomers for *N*-methylspiropyrrolidine **5**.

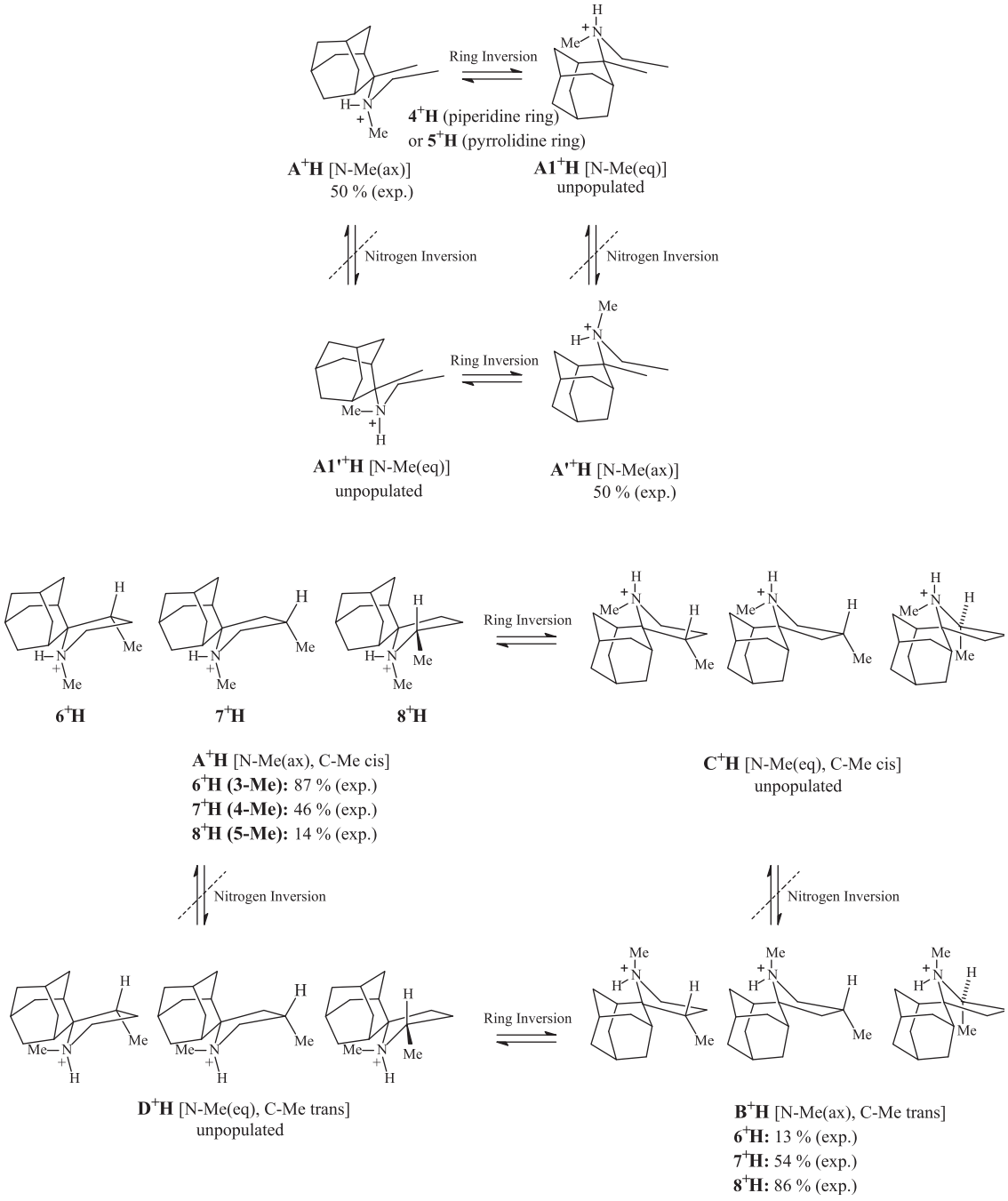

Scheme 4. Interconversion of different conformers for compounds **4**$^+$**H**–**8**$^+$**H** (experimental populations are given).

2. Results and discussion

2.1. Populated conformers

The protonation experiments for the *N*-Me, *C*-Me spiropyrrolidines **6**–**8** showed directly that two of the possible four conformers **A**–**D** are populated for each compound while for compounds **4**, **5** the two conformational enantiomers **A**, **A**′ are populated. In this experiment, rapid irreversible protonation of the *N*-Me derivatives **4**–**8** led to a mixture of the enantiomeric (**4**$^+$**H** and **5**$^+$**H**) or diastereomeric salts (**6**$^+$**H**, **7**$^+$**H** and **8**$^+$**H**). The new conformational diagram is shown in Scheme 4, with passage from the left to the right representing dissociation/reassociation of a proton. This is slow even at room temperature, so two sets of signals are seen for **6**–**8**, one corresponding to the stereoisomer of the left-hand side and the other to the stereoisomer of the right-hand side, and their relative abundance reflects approximately the relative abundance of free amines that existed before addition of the acid;[14] for compounds **4**,**5** the enantiomers **A**,**A**′ are populated giving rise to one set of signals. Energy calculations of the optimized structures will be discussed first as they illustrate the range of conformational possibilities.

2.1.1. Calculations. Four conformers are possible for the protonated spiropyrrolidines **6**$^+$**H**, **7**$^+$**H** and **8**$^+$**H**, i.e., **A**$^+$**H** [*N*-Me(ax), *C*-Me(cis)], **B**$^+$**H** [*N*-Me(ax), *C*-Me(trans)], **C**$^+$**H** [*N*-Me(eq), *C*-Me(cis)] and **D**$^+$**H** [*N*-Me(ax), *C*-Me(trans)] (Scheme 4). For compounds **4**$^+$**H** and **5**$^+$**H** the relevant conformers are the pairs of the two

Table 1
Structure calculations at different levels of theory (MM3, B3LYP/6-31+G** and MP2/6-311++G**//B3LYP/6-31+G**) and experimental results for the low energy conformational stereoisomers of the compounds **4**$^+$**H**, **5**$^+$**H** and **6**$^+$**H**–**8**$^+$**H**

Conformer	Description	Calculated relative energy (kcal mol^{-1})		Experimental % population[a] (298 K)	
		4$^+$**H**	**5**$^+$**H**	**4**$^+$**H**	**5**$^+$**H**
A$^+$**H**	*N*-Me(ax)	0.00 (MM3) 0.00 (B3LYP) 0.00 (MP2)	0.00 (MM3) 0.00 (B3LYP) 0.013 (MP2)	50%	50%
A′$^+$**H**	*N*-Me(ax)	0.00 (MM3) 0.00 (B3LYP) 0.00 (MP2)	0.00 (MM3) 0.00 (B3LYP) 0.00 (MP2)	50%	50%
A1$^+$**H**	*N*-Me(eq)	8.34 (MM3) 9.42 (B3LYP) 10.61 (MP2)	5.21 (MM3) 6.34 (B3LYP) 7.42 (MP2)	Unpopulated[b]	Unpopulated
A1′$^+$**H**	*N*-Me(eq)	8.34 (MM3) 9.42 (B3LYP) 10.61 (MP2)	5.21 (MM3) 6.34 (B3LYP) 7.42 (MP2)	Unpopulated[b]	Unpopulated

Conformer	Description	Relative energy (kcal mol^{-1})					
		Calculated			Experimental (% population at 298 K)[a]		
		6$^+$**H**	**7**$^+$**H**	**8**$^+$**H**	**6**$^+$**H**	**7**$^+$**H**	**8**+**H**
A$^+$**H**	*N*-Me(ax), *C*-Me(cis)	0.00 (MM3) 0.00 (B3LYP) 0.00 (MP2)	0.00 (MM3) 0.00 (B3LYP) 0.013 (MP2)	0.77 (MM3) 0.34 (B3LYP) 0.52 (MP2)	0.00 (87%)	0.09 (46%)	1.07 (14%)
B$^+$**H**	*N*-Me(ax), *C*-Me(trans)	1.86 (MM3) 2.53 (B3LYP) 2.60 (MP2)	0.22 (MM3) 0.25 (B3LYP) 0.00 (MP2)	0.00 (MM3) 0.00 (B3LYP) 0.00 (MP2)	1.13 (13%)	0.00 (54%)	0.00 (86%)
C$^+$**H**	*N*-Me(eq), *C*-Me(cis)	—[c] (MM3) —[c] (B3LYP) —[c] (MP2)	5.73 (MM3) 7.12 (B3LYP) 8.11 (MP2)	6.85 (MM3) 7.94 (B3LYP) 8.64 (MP2)	Unpopulated[b]	Unpopulated	Unpopulated
D$^+$**H**	*N*-Me(eq), *C*-Me(trans)	2.41 (MM3) 5.04 (B3LYP) 5.28 (MP2)	4.84 (MM3) 5.80 (B3LYP) 6.99 (MP2)	4.34 (MM3) 5.12 (B3LYP) 6.04 (MP2)	Unpopulated	Unpopulated	Unpopulated

[a] The relative populations were calculated at T=298 K using equation ΔG^0(cal mol^{-1})=−1.9872Tln K_{eq}, which is derived from ΔG^0=−RTln K_{eq} after units conversion.
[b] Conformers **C**$^+$**H**, **D**$^+$**H** for compounds **6**$^+$**H**–**8**$^+$**H** and **A1′**$^+$**H** for compounds **4**$^+$**H**, **5**$^+$**H** with an *N*-Me(eq) orientation are much more than 2.7 kcal mol^{-1} above the global minimum and are considered to be unpopulated (see Ref. 5b).
[c] Resulting to conformer **A** during minimization.

enantiomeric forms **A**$^+$**H**, **A′**$^+$**H** with *N*-Me(ax) and **A1**$^+$**H**, **A1′**$^+$**H** with *N*-Me(eq).

Different levels of theory[15] were tested, i.e., the force field MM3(96), which is parameterized for ammonium groups, the B3LYP density functional and the 6-31+G** basis set and the MP2/6-311++G**//B3LYP/6-31+G** method for a more accurate consideration of electron correlation. The relative energies of the conformers are depicted in Table 1.

The conformational enantiomers **A**$^+$**H**, **A′**$^+$**H** with the *N*-Me group axial were predicted to be the only populated species for spiropiperidine **4**$^+$**H** and spiropyrrolidine **5**$^+$**H**. The calculations located the two conformational diastereomers **A**$^+$**H** and **B**$^+$**H** as populated structures for compounds **6**$^+$**H**, **7**$^+$**H** and **8**$^+$**H**. The conformation **A**$^+$**H** with the *N*-Me axial and the *C*-Me cis to the *N*-Me group was calculated to be the most stable for compound **6**$^+$**H**; conformer **B**$^+$**H** with the *N*-Me axial and the *C*-Me trans to the *N*-Me group is less favoured because of the steric crowding between adamantane and *C*-Me. In compound **8** conformer **A**$^+$**H** is destabilized with respect to **B**$^+$**H** because of the *gauche* repulsive interaction between the *N*-Me and *C*-Me groups. In **7**$^+$**H** species, **A**$^+$**H** and **B**$^+$**H** were calculated to be equally populated, with **B**$^+$**H** having a slightly lower energy than **A**$^+$**H** according to the electron correlated MP2 level, which was the highest level of theory used; in **7**$^+$**H**, *C*-Me is attached at the pyrrolidine C-4 position and no significant steric repulsions arise between the two methyl groups or between *C*-Me and the adamantane entity.

The calculations predicted that all conformers with the *N*-Me group in an equatorial position, i.e., **C**$^+$**H**, **D**$^+$**H**, for **6**$^+$**H**–**8**$^+$**H**, and **A1**$^+$**H**, **A1′**$^+$**H**, for **4**$^+$**H**, **5**$^+$**H**, are unpopulated because of the severe steric crowding between adamantane and the *N*-Me group (Table 1). The NOE experiments also provide experimental evidence for the conformational characteristics of the compounds under study (see Supplementary data). The main conclusions of the calculations for compounds **4**$^+$**H**–**8**$^+$**H** will be useful in the discussion later.

2.1.2. NMR experiments. By addition of a drop of trifluoroacetic acid to the NMR tube, two sets of signals were observed in the NMR spectra of the protonated forms **6**$^+$**H**, **7**$^+$**H** and **8**$^+$**H** (see Fig. 1 for compound **8**$^+$**H** and Figs. S1 and S2 in Supplementary data for compounds **6**$^+$**H** and **7**$^+$**H**) corresponding to the diastereomeric conformations **A**$^+$**H** and **B**$^+$**H** according to the results of the calculations described above (see also Table 1). For **4**$^+$**H** and **5**$^+$**H** the enantiomeric structures **A**$^+$**H** and **A′**$^+$**H** are formed with identical NMR spectra. However, each of the peaks corresponding to the carbons 1′,3′-C or 4′,9′-C or 8′,10′-C was split into two signals because carbons of each pair become diastereotopic after protonation; in Figure 2 this part of the ^{13}C NMR spectrum for the spiropyrrolidine **5**, before and after TFA addition, is shown representatively.

The relative population **A**$^+$**H**/**B**$^+$**H** was estimated through measuring the relative signal intensities. The *N*-Me or *C*-Me pair of peaks in the ^{1}H NMR spectra and several pairs in the ^{13}C NMR spectra were offered for estimating the ratio **A**$^+$**H**/**B**$^+$**H**. For the compounds **6**$^+$**H**, **7**$^+$**H** and **8**$^+$**H** the ratio **A**$^+$**H**/**B**$^+$**H** was 87:13, 46:54 and 14:86, respectively (Fig. 1, Figs. S1 and S2 in Supplementary data and Scheme 4) corresponding to the free energy differences $\Delta G^0_{298\ K}$=1.13, −0.09 and −1.07 kcal mol^{-1}, respectively, compared with the experimental results the calculated values are of fair accuracy (see Table 1).

2.2. Nitrogen inversion process in spiro[pyrrolidine-2,2′-adamantanes] 5–8

*2.2.1. Dynamic NMR study of N-methylspiro[pyrrolidine-2,2′-adamantane] **5**.* The stereomutation process shown in Scheme 3 can be

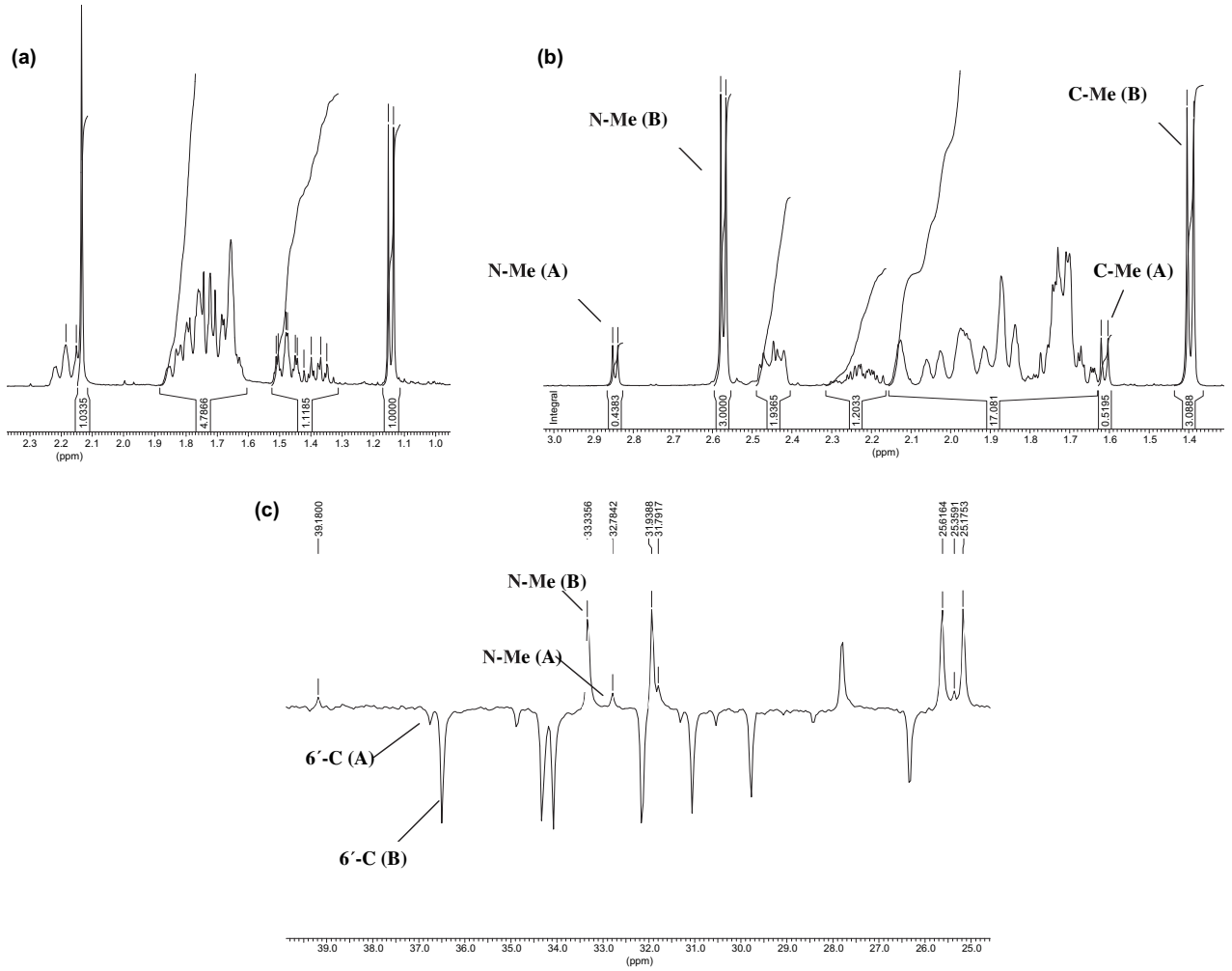

Figure 1. (a) Region of the ^{1}H NMR spectrum of the 1,5-dimethylspiro[pyrrolidine-2,2′-adamantane] **8** in a $CDCl_3$ solution (400 MHz) at 298 K; (b), (c) region of the ^{1}H NMR at 400 MHz and region of the ^{13}C NMR (DEPT) spectrum at 50 MHz (bottom part) in a $CDCl_3$ solution of compound **8** after adding a drop of trifluoroacetic acid to the NMR tube at 298 K. Some signals of the major conformer $\mathbf{B}^{+}\mathbf{H}$ and the minor conformer $\mathbf{A}^{+}\mathbf{H}$ are annotated.

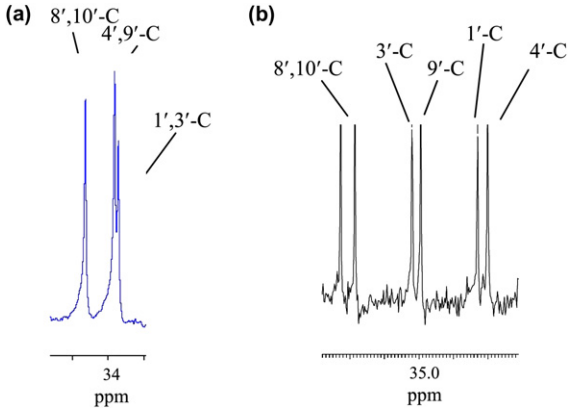

Figure 2. (a) Region of the ^{13}C NMR spectrum (50 MHz) of the *N*-methylspiro-[pyrrolidine-2,2′-adamantane] **5** in a $CDCl_3$ solution at 298 K before and (b) after adding a drop of trifluoroacetic acid to the NMR tube.

monitored at a non-chiral environment using adamantane as a prochiral probe;[16] at low temperatures the rate of exchange becomes slow on the NMR time scale and each of the three resonances corresponding to the carbon pairs 1′,3′-C, 4′,9′-C and 8′,10′-C is expected to be split into two signals, yielding six peaks.

The ^{1}H and ^{13}C NMR spectra of compound **5** in CD_2Cl_2 solution were temperature dependent, showing broadening and splitting of signals as the sample temperature was lowered.[17] The process was more clearly observed in the variable temperature ^{13}C NMR spectrum due to its better dispersion. Each of the signals corresponding to the carbon pairs 4′,9′-C, 8′,10′-C and 1′,3′-C was significantly broadened at temperatures between 298 K and 183 K; carbons of each pair were equivalent at the ambient temperature spectrum. Decoalescence was observed for the resonance of carbons 8′,10′ at about 188 K and at 183 K two signals of equal intensity were observed (Fig. 3).

According to the dynamic NMR theory for a symmetrical two site process, at the temperature of maximum broadening the two enantiomers are interconverted with a rate constant $k=2.2\Delta\nu$, where $\Delta\nu$ is the peak separation. For the peaks of carbonyl 8′-C and 10′-C, $\Delta\nu=53.2$ Hz (100 MHz) at 183 K and $k=117.0$ s^{-1}. Using these data and the Eyring equation, the free energy of activation $\Delta G^{\#}_{188K}$ for NI was calculated to be 9.1 kcal mol^{-1} at $T_c=188$ K.[17]

2.2.2. Calculations of NI barriers. The experimental and calculated NI barrier ax→ts for the *N*-methylspiropyrrolidine **5**, which corresponds to the energy difference between the transition state with a planar nitrogen geometry and the ground state axial conformer, were compared at some levels of theory. Using the B3LYP/6-31+G**, B3LYP/6-311++G**//B3LYP/6-31+G** and B3LYP/6-311++G** methods, the calculated values were 5.68, 5.61 and 5.67 kcal mol^{-1}, that is, 4.4 kcal mol^{-1} smaller than that of the experimental value. However, the MP2/6-311++G**//B3LYP/6-31+G** calculated energy was

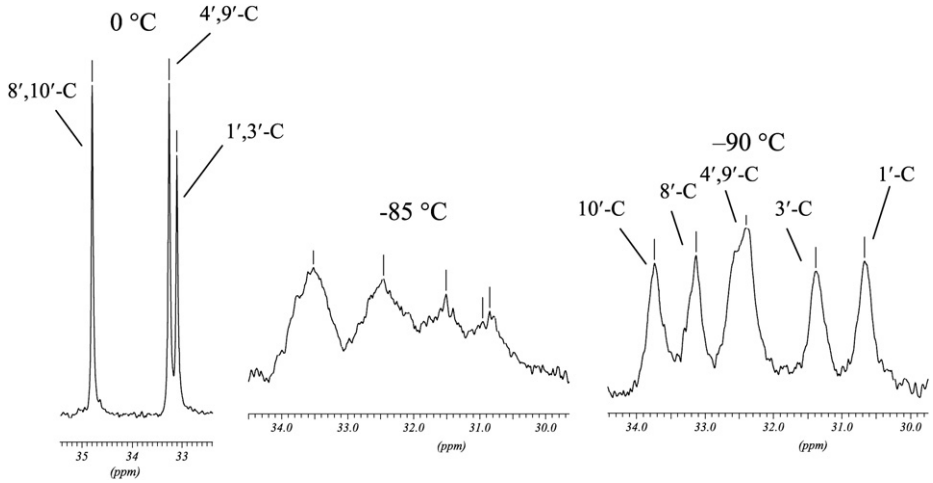

Figure 3. Part of the ^{13}C NMR spectra of the *N*-methylspiropyrrolidine **5** in a CD_2Cl_2 solution (100 MHz) at 273, 188 and 183 K; at 183 K signals splitting was observed because nitrogen inversion became a slow process at this temperature.

8.35 kcal mol^{-1}, which agrees acceptably with the experimental value of 9.1 kcal mol^{-1}; in addition the calculated energy values for the NI process eq→ts of the *N*-methylpyrrolidine and *N*-methylpiperidine at the MP2/6-311++G**//B3LYP/6-31+G** theory level were calculated to be 7.25 and 8.08 kcal mol^{-1}, respectively, which are in good agreement with the experimental values of 7.2 and 8.7 kcal mol^{-1}, respectively.[13] Good results were obtained recently from calculations at the MP2/6-31G* level for some cyclic amines, i.e., the difference between the experimental and calculated values for the NI barrier heights was less than 0.9 kcal/mol.[18] These results suggest that the MP2/6-311++G**//B3LYP/6-31+G** calculated NI ax→ts barriers for compounds **4**–**8** (Table 2) can be used as good approximations of the experimental ones.

Table 2
MP2/6-311++G**//B3LYP/6-31+G** calculated nitrogen inversion barriers ax→ts for the *N*-methylpyrrolidine, the *N*-methylpiperidine and their spiroadamantane derivatives **4**–**8**; some available experimental values are also included

Compound	Nitrogen inversion	Barrier height (kcal mol^{-1})	
	Description[a,b]	Calculated	Experimental
N-Methylpyrrolidine	*N*-Me(ax)→ts	7.25	7.2
N-Methylpiperidine	*N*-Me(ax)→ts	8.08	8.7
4	*N*-Me(ax): **A** or **A′**→ts or ts′	9.53	—[c]
5	*N*-Me(ax): **A** or **A′**→ts or ts′	8.35	9.1
6	*N*-Me(ax), *C*-Me cis: ***A***→ts	4.61	—
	N-Me(ax), *C*-Me trans: **B**→ts′	11.20	
7	*N*-Me(ax), *C*-Me cis: **A**→ts	7.96	—
	N-Me(ax), *C*-Me trans: ***B***→ts′	9.17	
8	*N*-Me(ax), *C*-Me cis: **A**→ts	7.09	—
	N-Me(ax), *C*-Me trans: ***B***→ts′	6.33	

[a] The transition state (ts) structures have a planar nitrogen geometry.
[b] Frequency calculations ensure that conformers **A** and **B** represent minima and that ts correspond to transition state structures.
[c] For compound **4** the experimental barrier for ax→[eq]→ax′ enantiomerization was 15.2 kcal mol^{-1} corresponding to a rate determining ring inversion process; for compounds **6**–**8** the bold italicized conformers indicate the global minima.

Prime MM3 calculations located the *N*-Me(eq) conformer of *N*-methylspiropiperidine **4**, 8.34 kcal mol^{-1} above the *N*-Me(ax) conformer (the calculated value at the MP2/6-311++G**//B3LYP/6-31+G** level is 10.61 kcal mol^{-1}) due to the severe steric crowding between the *N*-Me group and adamantane ring. Therefore, it was speculated that the rate of ax→[eq]→ax′ interconversion (Scheme 2) is controlled by an energy demanded N-inversion barrier, caused by the *N*-methyl group passing over the adamantane C4′$_{ax}$–H and C9′$_{ax}$–H bonds. However, the experimental enantiomerization barrier height ax→[eq]→ax′ of 9.10 kcal mol^{-1} for spiropyrrolidine **5**, corresponding to its nitrogen inversion barrier, is much smaller than that of spiropiperidine **4** (15.2 kcal mol^{-1}). Since compounds **4** and **5** have calculated nitrogen inversion barriers with close values, see Table 2, it is clear that RI and not NI is the rate determining process for the spiropiperidine **4**.

It is interesting to examine then, how the *C*-methyl substitution of compound **5** at the available positions of the pyrrolidine ring affects the NI barrier height of the *N*-methylpyrrolidine ring. In compounds **6**–**8**, the two populated diastereomeric conformers **A** and **B** can be interconverted through the two pathways **A**→ts→[**D**]→**B** or **B**→ts′→[**C**]→**A** (Schemes 4 and Scheme S1 in Supplementary data), which include successive NI and RI (pseudorotation) steps. In each of these pathways nitrogen inversion is the important process and the NI transition states ts and ts′ are diastereomeric; the relevant pathways **A**→ts→[**A1′**]→[**A′**] and **A′**→ts′→[**A1**]→[**A**] include the enantiomeric NI transition states ts and ts′. The calculations suggest that for compounds **6** and **8** the lowest in energy pathways include the transformations **A**→ts and **B**→ts′, respectively; in both cases the starting structure is the calculated global minimum (Table 2 and Table S1 in Supplementary data). For compound **7** the calculations predicted that **A**→ts is preferred; the starting structure conformer **A** is 0.16 kcal mol^{-1} higher in energy than the ground state structure **B**.

It is worth mentioned that in compounds **6**,**8** nitrogen inversion barrier height is decreased compared to that of **5** and the more dramatic change is noted for compound **6** with a barrier height of 4.61 kcal mol^{-1} (see Table 2); this is due to the destabilization of the ground state conformer in compound **6** resulting in the lowering of the barrier for the NI ax→ts process. Of the *C*-Me derivatives **6**–**8**, the global minimum in compound **6** bears the most significant steric repulsions resulted from the crowding between the two methyl groups having a relative 1,3-diaxial orientation; in the ground state conformer of compound **8** two *gauche* methyl groups are present. In compound **7** no significant steric repulsions are present and the nitrogen inversion barrier height is close to that of compound **5**.

Below it is summarized how the attachment of a spiroadamantane entity at the C-2 position influences the conformational preferences and the dynamic processes of the *N*-methylpyrrolidine and the *N*-methylpiperidine.

(a) The parent heterocycles *N*-methylpyrrolidine and *N*-methylpiperidine adopt a global minimum with an equatorial orientation of the *N*-Me group. The energy difference between the axial and the equatorial conformer for the *N*-methylpiperidine is ~2.7 kcal mol^{-1} (solution) or 3.1 kcal mol^{-1} (gas phase)[19]

corresponding to a maximum of 1% population for the axial conformer; for the *N*-methylpyrrolidine in the gas phase, the equatorial conformer is >1.3 kcal mol^{-1} more stable than the axial[20] corresponding to a population of >89%. Nitrogen inversion in spiropyrrolidine **5** or ring/nitrogen inversion in spiropiperidine **4** can flip the *N*-Me group to the equatorial position (see Schemes 2 and 3) but this conformer is completely unstable. In the *N*-Me(eq) conformer the N–CH_3 bond vector is bisecting the 1′–2′–3′–4′–5′–9′ cyclohexane ring sub-unit of adamantane resulting in severe steric repulsions between the *N*-Me and 4′ax,9′ax protons; the MP2/6-311++G**//B3LYP/6-31+G** calculations for the *N*-methyl spiropiperidine **4** and the *N*-methylspiropyrrolidine **5** located the equatorial conformer 9.25 and 6.03 kcal mol^{-1}, respectively, above the ground state axial conformer (Table S1 in Supplementary data).

In the *N*-methylspiropyrrolidines **5**–**8** and the *N*-methyl spiropiperidine **4** the *N*-methyl group is completely axial because the 1,5-interaction between adamantane and methyl group is much more conformation-determining than any preference for equatorial over axial location, which was calculated to predominate in the parent *N*-methyl or 2,2-dimethyl-*N*-methyl heterocycles.[21]

(b) It is striking that the attachment of the spiroadamantane entity results in the interconversion between the only populated enantiomeric *N*-Me(ax) conformers ax→[eq]→ax′; the interconversion eq→ax between the *N*-Me(eq) and *N*-Me(ax) conformers, which are both populated, is observed in the *N*-methylpyrrolidine or *N*-methylpiperidine.

(c) According to the results of the dynamic NMR spectroscopy the energy required for the nitrogen inversion eq→ax in the *N*-methylpyrrolidine,[13] which is the major dynamic process for this molecule, is 7.2 kcal mol^{-1} corresponding to the barrier eq→ts, whereas for the spiranic analogue **5** the nitrogen inversion requires experimentally 9.1 kcal mol^{-1} to mount the barrier ax→ts. Comparison of the two relevant NI barriers ax→ts for the *N*-methylpyrrolidine and its spiroadamantane analogue **5** reveals that the latter requires about 5 kcal mol^{-1} higher energy.[22,20b]

For the parent *N*-methylpiperidine the energetic requirements[23] for the ring inversion and nitrogen inversion processes eq→ax correspond to the experimental values of ~12 kcal mol^{-1} and 8.7 kcal mol^{-1}, respectively.[13] In the spiroadamantane analogue **4** of the *N*-methylpiperidine the rate of the enantiomerization process ax→[eq]→ax′ is determined by a ring inversion barrier height of about ~15 kcal mol^{-1}, i.e., 6 kcal mol^{-1} higher than the relevant barrier for the ring inversion process ax→eq in the *N*-Me piperidine. In the *N*-methylspiropiperidine **4** the calculated nitrogen inversion barrier ax→ts is 9.53 kcal mol^{-1} whereas the estimated experimental value for the relevant nitrogen inversion barrier[22] ax→ts in the *N*-methylpiperidine is ~6.0 kcal mol^{-1}.

(d) While an enantiomerization interconverts *N*-Me axial conformers **A** and **A**′ in spiropiperidine **5** and spiropyrrolidine **4**, substitution of the pyrrolidine ring of **5** with a *C*-Me group effects a diastereomerization between conformers **A** and **B** and reduces effectively the NI barrier.

3. Experimental

3.1. NMR data

NMR experiments were conducted (i) on a 400 MHz Bruker DRX-Avance operating at 400.13 MHz for obtaining the ^{1}H NMR spectra and at 100.61 MHz for the dynamic ^{13}C NMR spectra, with the probe temperature maintained using a BVT-3000 Bruker control unit and (ii) on a 200 MHz Bruker Avance operating at 50.32 MHz for the ^{13}C NMR spectra at 298 K. The ^{1}H NMR experiments were run at 298 K (400 MHz) by dissolving 5 mg of compound **4**–**8** in 0.5 mL of $CDCl_3$; the protonated samples were prepared by addition of a drop of trifluoroacetic acid to the $CDCl_3$ solution inside the NMR tube. The ^{13}C NMR experiments were run at 298 K (50 MHz) by dissolving 20–30 mg of the compound in 0.5 mL of $CDCl_3$. ^{1}H chemical shifts (δ) are reported in parts per million relative to the residual $CHCl_3$ signal at 7.26 ppm (s); ^{13}C chemical shifts (δ) are reported in parts per million relative to the $CDCl_3$ signal at 77.0 ppm (t).

The 1D ^{1}H spectra (400 MHz) were acquired using a spectral width of 12 ppm, 2 s relaxation delay between cycles, 16 transients, 32K data points zero-filled to 64K data points before Fourier transformation (FT) and baseline correction. The 1D ^{13}C spectra (50 MHz) were recorded using 3 s relaxation delay, 512 transients, 64K data points and 3 Hz line broadening prior to FT. DEPT-135 spectrum (50 MHz) was recorded using 2 s relaxation delay, 800 transients 32K data points and 3 Hz line broadening prior to FT. The assignments of ^{1}H and ^{13}C signals were achieved by the combined use of DEPT, 2D COSY and HMQC experiments; for the 2D NMR experiments the 400 MHz Bruker DRX-Avance machine was used. The 2D NOESY were run in $CDCl_3$ solutions (400 MHz) at a concentration of 0.02 M using a mixing time of 1.2 s. All data were collected using pulse sequence and routines provided in the Bruker library of pulse programs. Data processing was performed using the XWIN-NMR Bruker program.

The sample of compound **5** for low temperature experiments was prepared by dissolving **5** (80 mg) in CD_2Cl_2 (1 mL). The tube was then introduced into the precooled probe of the Bruker-DRX 400 MHz spectrometer operating at 400.13 for ^{1}H and 100.61 MHz for ^{13}C. ^{1}H chemical shifts (δ) are reported in parts per million relative to the residual $CHDCl_2$ signal at 5.32 ppm (s); ^{13}C chemical shifts (δ) are reported in parts per million relative to the CD_2Cl_2 signal at 53.8 ppm (quintet). The temperature was calibrated by means of a Ni/Cu thermocouple inserted into the NMR probe; the standard error in these kinetic studies using the coalescence method and approximate equations is not less that 0.5–0.7 kcal mol^{-1}. The experimental details for the synthesis of compounds will be discussed elsewhere.

3.2. Computations

All structures were fully optimized at the B3LYP/6-31+G**[15] level using the GAUSSIAN 03 package (for references of the structure calculations packages see Supplementary data) or with MM3(96) force field[15] using the PCMODEL package. Single point energy calculations were performed at the MP2/6-311++G** level.[15] Frequency calculations were performed at the B3LYP/6-31+G** level to characterize the stationary points, which are relevant to the nitrogen inversion process ax→ts for the compounds **4**–**8** (see Table 2) and the nitrogen inversion process eq→ts for the *N*-methylpyrrolidine and *N*-methylpiperidine.

Acknowledgements

This research was supported by a research grant from the Special Account for Research Grants of the National and Kapodistrian University of Athens, Greece (research program code 70/4/8775). I am grateful to Ioannis Stylianakis for his contribution to the experimental part of this study.

Supplementary data

Results of the NOE experiments, informative regions of spectra before and after the addition of TFA for compounds **6**, **7** (Figs. S1 and S2). Conformational diagrams for the free amines **4**–**8** (Scheme S1). Calculated relative stability of conformers **A**, **B** for free amines **6**–**8** (Table S1). Cartesian coordinates of the optimized conformers for **4**–**8** (protonated and neutral forms) at the B3LYP/6-31+G** level. References for structure calculations packages. Supplementary data

associated with this article can be found in the online version, at doi:10.1016/j.tet.2009.08.071.

References and notes

1. (a) Hay, A. J.; Wolstenholme, A. J.; Skehel, J. J.; Smith, M. H. *EMBO J.* **1985**, *4*, 3021; (b) Hay, A. J. *Semin. Virol.* **1992**, *3*, 21; (c) Pinto, L. H.; Holsinger, L. J.; Lamb, R. A. *Cell* **1992**, *69*, 517; (d) Stouffer, A. L.; Acharya, R,; Salom, D,; Levine, A. S.; Di Costanzo, L.; Soto, C. S.; Tereshko, V.; Nanda, V.; Stayrook, S.; DeGrado, W. *Nature* **2008**, *451*, 596.
2. Parsons, C. G.; Stöffler, A.; Danysz, W. *Neuropharmacology* **2007**, *53*, 699.
3. Some selected references are: (a) Kolocouris, N.; Foscolos, G. B.; Kolocouris, A.; Marakos, P.; Pouli, N.; Fytas, G.; Ikeda, S.; De Clercq, E. *J. Med. Chem.* **1994**, *37*, 2896; (b) Kolocouris, N.; Kolocouris, A.; Foscolos, G. B.; Fytas, G.; Neyts, J.; Padalko, E.; Balzarini, J.; Snoeck, R.; Andrei, G.; De Clercq, E. *J. Med. Chem.* **1996**, *39*, 3307; (c) Stylianakis, I.; Kolocouris, A.; Kolocouris, N.; Fytas, G.; Foscolos, G. B.; Padalko, E.; Neyts, J.; De Clercq, E. *Bioorg. Med. Chem. Lett.* **2003**, *13*, 1699; (d) Kolocouris, A.; Spearpoint, P.; Martin, S. R.; Hay, A. J.; López-Querol, M.; Sureda, F. X.; Padalko, E.; Neyts, J.; De Clercq, E. *Bioorg. Med. Chem. Lett.* **2008**, *18*, 6156.
4. (a) Kolocouris, A.; Hansen, R.; Broadhurst, R. W. *J. Med. Chem.* **2004**, *47*, 4975; (b) Broadhurst, R. W.; Kolocouris, A.; Zikos, C. *Bioorg. Med. Chem. Lett.* **2007**, *17*, 3947.
5. (a) Kolocouris, A.; Mikros, E.; Kolocouris, N. *J. Chem. Soc., Perkin Trans. 2* **1998**, 1701; (b) The notation 'unpopulated conformer' indicates a population of $\leq$1% for a minor conformer, which is considered to be the limit of observation in a DNMR study; this population corresponds to a $\sim$2.7 kcal mol^{-1} higher free energy from the global minimum (calculated using the equation ΔG^0(cal mol^{-1})$=-1.9872T\ln K_{eq}$).
6. Kolocouris, A.; Outeiriño, J. G.; Anderson, J. E.; Fytas, G.; Foscolos, G. B. *J. Org. Chem.* **2001**, *66*, 4989.
7. Kolocouris, A.; Ortore, G.; Martinelli, A., unpublished results.
8. Protons 4′$_{ax}$,9′$_{ax}$-H and 8′$_{ax}$,10′$_{ax}$-H have axial orientation relative to the 1′–2′–3′–4′–5′–9′ and the 1′–2′–3′–10′–7′–8′ cyclohexane ring sub-unit of adamantane, respectively (see Scheme 2).
9. Forsyth, D. A.; Zhang, W.; Hanley, J. A. *J. Org. Chem.* **1996**, *61*, 1284.
10. The force field calculations suggested that ring inversion is the rate determining process including a 3,6-boat, *N*-Me(eq) transition state (which connects the two twist-boat minima TW3 and TW4) with an energy of 16.4 kcal mol^{-1} above the global minimum, which matches the experimental value for **4**; in this structure strong steric repulsive forces between piperidine 3$_{eq}$-H and 8′$_{ax}$ adamantane-H and between piperidine 6$_{ax}$-H and 3′$_{ax}$ adamantane-H raise the energy (see Ref. 5a).
11. A C–X$\cdots$Y–C contact is considered to include van der Waals or steric repulsion (Pauli repulsive forces) when the r_{X-Y} is smaller than the sum of the X and Y van der Waals radii. Still the most popular source of van der Waals radii is an article by Bondii, A. *J. Phys. Chem.* **1964**, *68*, 441 who gives the following values H: 1.20 Å, C: 1.70 Å, O: 1.52 Å, N: 1.55 Å, F: 1.47 Å, Cl: 1.75 Å, S: 1.80 Å, P: 1.80 Å.; Si: 2.10 Å; using these values the sum of the van der Waals radii is for example 2.75 Å for H$\cdots$N and 2.40 Å for H$\cdots$H. The contacts between the *N*-Me(eq) group and adamantane ring in compounds **4** and **5** include such short H$\cdots$H distances as 2.03 Å and 1.84 Å, respectively, between the N–CH$_3$ and 9′ax-H protons; these values are much smaller than the sum of the van der Waals radii of H suggesting repulsive van der Waals forces.
12. (a) Crabb, T. A.; Katritzky, A. R. *Adv. Heterocycl. Chem.* **1984**, *36*, 1; (b) Nelsen, S. F.; Ippoliti, J. T.; Frigo, T. B.; Petillo, P. A. *J. Am. Chem. Soc.* **1989**, *111*, 1776.
13. (a) Belostotskii, A. M.; Aped, P.; Hassner, A. *J. Mol. Struct. (Theochem)* **1998**, *429*, 265; (b) Nelsen, S. F.; Ippoliti, J. T.; Frigo, T. B.; Petillo, P. A. *J. Am. Chem. Soc.* **1989**, *111*, 1776.
14. Eliel, E. L.; Kandamasy, D.; Yen, C. Y.; Hargrave, K. D. *J. Am. Chem. Soc.* **1980**, *102*, 3698.
15. MM3(96): see Allinger, N. L.; Yuh, Y. H.; Lii, J.-H. *J. Am. Chem. Soc.* **1989**, *111*, 8551 and; Lii, J.-H.; Allinger, N. L. *J. Phys. Org. Chem.* **1994**, *7*, 591; B3LYP: Becke, A. *J. Chem. Phys.* **1993**, *98*, 5648; MP2: Head-Gordon, M.; Pople, J. A.; Frisch, M. J. *Chem. Phys. Lett.* **1988**, *153*, 503; 6-31+G**, 6-311++G** are Pople basis sets, see: Frisch, M. J.; Pople, J. A.; Binkley, J. S. *J. Chem. Phys.* **1984**, *80*, 3265.
16. Mislow, K. *Top. Stereochem.* **1967**, *1*, 1.
17. Sandstrom, J. *Dynamic NMR Spectroscopy*; Academic: London, 1982.
18. Belostotskii, A. M.; Gottlieb, H. E.; Shokhen, M. *J. Org. Chem.* **2002**, *67*, 9257.
19. Crowley, P. J.; Robinson, M. J. T.; Ward, M. G. *Tetrahedron* **1977**, *33*, 915.
20. (a) Plafferott, G.; Oberhammer, H.; Boggs, J. E.; Caminati, W. *J. Am. Chem. Soc.* **1985**, *107*, 2305; (b) The calculations at MM2, MM3 and MP2/6-311++G**//B3LYP/6-31+G** suggest that the *N*-Me(ax) pyrrolidine conformer is 2.07, 2.98 and 3.04 kcal mol^{-1}, respectively, less stable than the equatorial.
21. Unpublished results.
22. An estimation of the NI ax$\rightarrow$ts barrier height, for the *N*-methylpyrrolidine and the *N*-methylpiperidine is obtained through substraction of the experimental conformational energy difference from the relevant experimental barrier height; for the *N*-methylpyrrolidine the relevant values can be found in Ref. 13; for the *N*-methylpiperidine see Refs. 13 and 19.
23. (a) The solution phase value for the ring inversion barrier is 11.8 kcal mol^{-1}: Lambert, J. B.; Kesge, R. G.; Carhart, R. E.; Jovanovich, A. P. *J. Am. Chem. Soc.* **1967**, *89*, 3761; (b) The gas phase value is 12.0 kcal mol^{-1}: Tafazzoli, M.; Suarez, C.; True, N. S.; LeMaster, C. B.; LeMaster, C. L. *J. Phys. Chem.* **1992**, *96*, 10201.